SIMULATION OF THE SMALL-SCALE DUST ACTIVITIES AND THEIR MUTUAL INTERACTIONS ON THE ATMOSPHERIC DYNAMICS USING A HIGH-RESOLUTION MARS GENERAL CIRCULATION MODEL. T. Kuroda[1,2] and M. Kadowaki[3], [1]National Institute of Information and Communications Technology (4-2-1 Nukui-Kitamachi, Koganei, Tokyo 184-8795 Japan, tkuroda@nict.go.jp), [2]Department of Geophysics, Tohoku University (6-3 Aramaki-aza-Aoba, Aoba, Sendai 980-8578 Japan), [3]Nuclear Science Research Institute, Japan Atomic Energy Agency (2-4 Shirane Shirakata, Tokai-mura, Naka-gun, Ibaraki 319-1195 Japan).

Introduction: It is well known that there are various scales of dust activities, from the small-scale 'dust devil' [1] to the global dust storm [2], in the Martian atmosphere. The dust cycle on Mars is similar to the water cycle on Earth; in which airborne dust absorbs solar radiation and emits in the infrared, and the created local heating and cooling affect the atmospheric dynamics at various scales [3].

Regional dust storms occur due to the strong wind stress on surface [4], mainly at sloped regions and edge of seasonal polar caps [5] possibly induced by thermal tide [6] and fromtal activities [7]. Also, dust is thought to be continuously supplied to the atmosphere by convective activities [8]. Recent studies indicate that such dust activities may induce the gravity waves (GWs) which strongly affect the dynamical features in thermosphere [9,10].

The theories of dust lifting (effects of surface wind stress and small-scale convection) have been parameterlized and implemented into Mars general circulation models (MGCMs) [11-13]. But the mutual impacts between small-scale dust activities and global-scale dynamical features have not been well investigated as the horizontal resolutions of those MGCMs were low (grid interval of ~5° or ~300 km). In this study we implement the parameterizations into our high-resolution (T106, grid interval of ~1.1° or ~67 km) MGCM [14,15] to investigate the mechanisms of the occurrence of local dust storms and their impacts on the generation of GWs.

Model Description: Our MGCM, DRAMATIC (Dynamics, RAdiation, MAterial Transport and their mutual InteraCtions) has been developed based on the CCSR/NIES/ FRCGC MIROC model [16] with a spectral solver for the three-dimensional primitive equations, on which the physical parameters (surface topography, albedo, thermal inertia) and processes (condensation of CO_2 gas, snowfall and generation of seasonal polar caps) have been implemented [17,18]. In the vertical direction, the model domain extends from the surface to ~80–100 km and is represented by 49 sigma-levels. The MGCM utilizes the LTE radiation scheme for CO_2 molecules in infrared (including the 15 μm band) and near-infrared, and radiative effects of dust from ulterviolet to far-infrared.

In this study we have implemented the dust lifting scheme which accounts for the lifting, transport by local winds and gravitational sedimentation [19]. The change of dust distribution by the scheme is interactive with the radiative calculations, which provides the feedback to the atmospheric wind and temperature. Dust is injected into the atmosphere by the parameterizatios of two processes: wind stress and convection.

Wind stress parameterization. The wind stress for the dust lifting, τ, is defined as follows:

$$\tau = \rho C_M^* \left(\frac{ku(z_1)}{\ln(z_1/z_0)} \right)^2,$$

Where ρ is the atmospheric density, $u(z_1)$ is the wind velocity at the lowest layer of atmosphere (z_1~50 m height), z_0 is the surface roughness [20], and k = 0.4 is the von Karman's constant. C_M^* is the stability function of momentum which is a function of the Richardson number Ri. C_M^* is defined as follows [21],

$$C_M^* = \frac{1}{\left(1 + 10Ri/\sqrt{1+5Ri}\right)^2} \quad (Ri > 0),$$

$$C_M^* = 1 - 64Ri \quad (Ri \le 0).$$

The dust flux from the surface due to wind stress, F_{wsl} (in kg m^{-2} s^{-1}), is defined as follows [11],

$$F_{wsl} = \max\left[\alpha_N \frac{2.61}{g\sqrt{\rho}} \left(\sqrt{\tau} - \sqrt{\tau^*}\right)\left(\sqrt{\tau} + \sqrt{\tau^*}\right)^2, 0 \right],$$

where g is the gravitational acceleration, α_N is the lifting efficiency and τ^* is the threshold wind stress for lifting. In this study α_N and τ^* are set to be the order of 10^{-7} m^{-1} and 0.05 N m^{-2}, respectively.

Convective parameterization. The dust flux from the surface due to small-scale convective motions (dust devil), F_{dda} (in kg m^{-2} s^{-1}), is defined as follows [11],

$$F_{dda} = \max[\alpha_D \tau_H (1-b), 0],$$

where α_D is the lifting efficiency (set to be the order of 10^{-10} kg J^{-1} in this study), and τ_H is the sensible heat flux on the ground. b is defined as follows [8],

$$b = \frac{(1-\zeta^{\kappa+1})}{(1-\zeta)(\kappa+1)\zeta^{\kappa}},$$

where ζ is the ratio of pressure at the top of planetary boundary layer (PBL) divided by the surface pressure, and $\kappa = R/c_p$is the specific gas constant divided by the specific heat capacity at constant pressure. τ_H (in W m^{-2}) is defined as follows,

$$\tau_H = \rho c_p \sqrt{C_M^* C_H^*} \left(\frac{k}{\ln(z_1/z_0)}\right)^2 u(z_1)(\theta_0 - \theta_1),$$

where θ_0 and θ_1 are the ground surface temperature and the potential temperature of the lowest layer of atmosphere, respectively. C_H^*, the stability function of heat, is defined as follows [21],

$$C_H^* = \frac{1}{\left(1+15Ri/\sqrt{1+5Ri}\right)^2} \quad (Ri > 0),$$

$$C_H^* = 1 - 16Ri \quad (Ri \le 0).$$

With the fluxes $F_{wsl} + F_{dda}$, dust is supplied from the ground surface up to the top of PBL uniformly. The vertical extent of PBL is assumed from the static stability S defined with the vertical temperature gradient dT/dz as follows,

$$S = \frac{dT}{dz} + \frac{g}{c_p}.$$

The altitude at which the static stability abruptly changes is assumed as the top of the PBL. Dust is assumed to be able to lift from the ground infinitely, and no dust lift occurs from the seasonal polar caps.

Gravitational sedimentation of the airborne dust particles is implemented into the model assuming the pure CO_2 atmosphere [18,22]. The density and average radius of dust are set to be 2500 kg m^{-3} and ~1.26 μm (to be consistent with the dust particle size assumed in the radiation scheme [23]), respectively.

Preliminary Results: Figures 1-3 show the simulated day-mean dust opacity (in visible wavelength) and dust fluxes from the surface due to wind stress (F_{wsl}) and convection (F_{dda}) at L_s=180° (northern autumn equinox). The dust opacity is in overall comparable to the past observations (e.g. MGS-TES). The lifting by wind stress tends to occur on slopes, especially around the mountains (Olympus and Elysium) and northern edge of the Hellas Basin. The lifting by convection uniformly occurs in low- and mid-latitudes.

In the presentation we plan to show more detailed results and analyses, e.g. results in other seasons/seasonal variances of dust conditions, key meteorological features for the lifting of dust, and generation of GWs due to local dust storms.

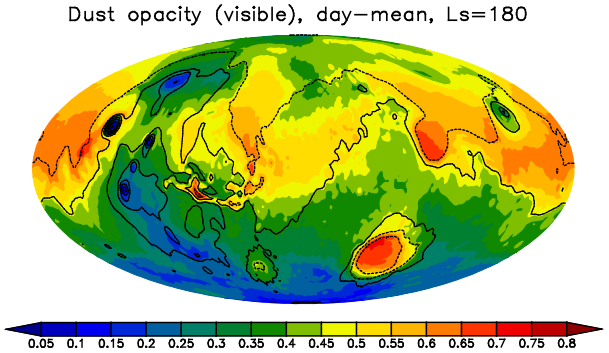

Figure 1: Horizontal distribution of day-mean dust opacity (in visible wavelength) simulated with our T106 MGCM at L_s=180° (northern autumn equinox).

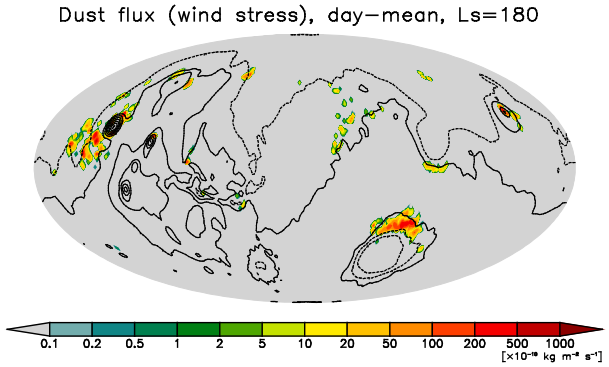

Figure 2: Same as Figure 1 but the distribution of F_{wsl} (in kg m^{-2} s^{-1}).

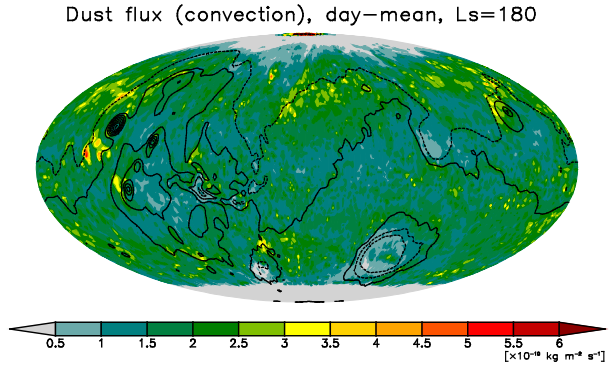

Figure 3: Same as Figure 1 but the distribution of F_{dda} (in kg m^{-2} s^{-1}).

References: [1] Greeley R. et al. (2006) *JGR, 111,* E12S09. [2] Smith M.D. et al. (2002) *Icarus, 157,* 259–263. [3] Medvedev A.S. et al. (2011) *Aeolian Res., 3,* 145–156. [4] Greeley R. and Iversen J.D. (1985) Cambridge University Press. [5] Cantor B.A. et al. (2001) *JGR, 106,* 23653–23687. [6] Leovy C.B. and Zurek R.W. (1979) *JGR, 84,* 2956–2968. [7] Wang H. et al. (2005) *JGR, 110,* E07005. [8] Rennó N.O. et al. (1998) *JAS, 55,* 3244–3252; [9] Spiga A. et al. (2013) *JGR, 118,* 746–767. [10] Imamura T. et al. (2016) *Icarus, 267,* 51–63. [11] Newman C.E. et al. (2002) *JGR, 107*(E12), 5123. [12] Basu S. et al. (2004) *JGR, 109,* E11006. [13] Kahre M.A. et al. (2006), *JGR, 111,* E06008. [14] Kuroda T. et al. (2015) *GRL, 42,* 9213–9222. [15] Kuroda T. et al. (2016) JAS, 73, 4895–4909. [16] K-1 Model Developer (2004) *K-1 Tech. Rep., 1,* 1–34, Univ. of Tokyo. [17] Kuroda T. et al. (2005) *J. Meteor. Soc. Japan, 83,* 1–19. [18] Kuroda T. et al. (2013) *GRL, 40,* 1484–1488. [19] Kadowaki M. (2014) Ph.D. dissertation, Univ. of Tokyo. [20] Heavens N.G. et al. (2008) *JGR, 113,* E02014. [21] Haberle R.M. et al. (1999) *JGR, 104,* 8957–8974. [22] Kasten F. (1968) *J. Appl. Meteor., 7,* 944–947. [23] Tomasko M.G. et al. (1999) *JGR, 104,* 8987–9007.